



Published in final edited form as:

*Semin Nucl Med.* 2018 May ; 48(3): 242–245. doi:10.1053/j.semnuclmed.2017.12.002.

## Imaging Macrophage-associated Inflammation

Catherine A. Foss, PhD<sup>\*,†</sup>, Julian Sanchez-Bautista, MD<sup>†,‡</sup>, and Sanjay K. Jain, MD<sup>†,‡</sup>

<sup>\*</sup>Russell H. Morgan Department of Radiology and Radiological Sciences, Johns Hopkins University School of Medicine, Baltimore, MD

<sup>†</sup>Center for Infection and Inflammation Imaging Research, Johns Hopkins University School of Medicine, Baltimore, MD

<sup>‡</sup>Department of Pediatrics, Johns Hopkins University School of Medicine, Baltimore, MD

### Abstract

Macrophages belong to the mononuclear phagocyte system comprising closely related cells of bone marrow origin. Activated macrophages are critical in several diseases such as tuberculosis, sarcoidosis, Crohn's disease, and atherosclerosis. Noninvasive imaging techniques that can specifically image activated macrophages could therefore help in differentiating various forms of inflammatory diseases and to monitor therapeutic responses.

### Introduction

Macrophages mediate an innate immune response of inflammation, being one of the first lines of defense against the invasion of various pathogens, as well as in several chronic inflammatory diseases.<sup>1</sup> Various nuclear imaging techniques are currently in development, and we discuss some of the promising targets and agents in this review.

### Imaging Folate Receptor (FR)- $\beta$

FRs are cell surface glycoproteins of molecular weights in the range of 38–45 kDa and attach to the plasma membrane by a glycosylphosphatidylinositol anchor.<sup>2</sup> Several isoforms are present in humans and include FR- $\alpha$ , FR- $\beta$ , and FR- $\gamma$ . FR- $\beta$  is a marker protein in normal hematopoiesis in the lineage of myelomonocytic cells,<sup>2</sup> and is also found in pathogenic cells, such as acute and chronic myelogenous leukemia cells.<sup>3</sup> FR- $\beta$  is overexpressed on activated but not normal macrophages, and its expression on other cells is undetectable,<sup>4</sup> making this receptor a good target for imaging macrophage-mediated inflammatory diseases. The diagnostic and therapeutic implications of this target were demonstrated by Chandrupatla et al, where they highlighted the role of <sup>18</sup>F-fluoro-PEG-folate PET as a therapeutic monitoring tool for methotrexate therapy.<sup>5</sup>

Small molecule ligands that specifically target FR-beta have several advantages, including high affinity to its target even after conjugation, easy conjugation with imaging agents, and the low or undetectable expression of the target receptor on normal cells.<sup>4</sup> Folic acid has

Address reprint requests to: Sanjay K. Jain, MD, Department of Pediatrics, Johns Hopkins University School of Medicine, 1550 Orleans St, Rm 109, Baltimore, MD 21287. sjain5@jhmi.edu.

been linked to a variety of dyes or radiopharmaceuticals, such as  $^{99m}\text{Tc}$ , gallium-67, and indium-111, and have been used for imaging in the detection of FR-positive activated macrophages and cancer cells.<sup>1,6-8</sup> In addition, in carotid endarterectomy specimens of 20 patients, higher numbers of M2-like macrophages were present in areas of high  $^{99m}\text{Tc}$ -folate accumulation than in areas with low accumulation, suggesting that this technique can also detect pathologies caused by M2-like macrophage phenotypes.<sup>9</sup> Imaging studies of macrophage-mediated inflammatory diseases using FR- $\beta$  have been performed in animals models and in human patients (Table).

### Imaging CD206, the Mannose Receptor

The mannose receptor (MRC-1, CD206) is a C-type lectin primarily present on the surface of macrophages and immature dendritic cells. CD206 mediates the endocytosis of glycoproteins by macrophages but also acts as a phagocytic receptor for bacteria, fungi, and other pathogens.<sup>17,18</sup> However, mannose receptor expression is not macrophage restricted; it is also expressed by hepatic and lymphatic endothelia, and dendritic and kidney mesangial cells.<sup>19</sup> MRC-1-targeting agents are mostly designed for imaging tumor-associated macrophages and other macrophage-mediated diseases like rheumatoid arthritis. Nanobodies against the macrophage mannose receptor have been developed and were successfully used to specifically target a subpopulation of tumor-infiltrating macrophages in SPECT-micro-CT imaging studies.<sup>20,21</sup> However, Bala et al found no significant uptake of MRC-specific nanobodies in atherosclerotic lesions in a mouse model.<sup>22</sup>

### Imaging the Translocator Protein (TSPO)

Monocytes and their progeny (macrophages, microglia, and dendrocytes) express the TSPO along with many other cell types, notably the heart, lung, kidney, endocrine tissues, and endothelium. TSPO is an 18-kD transmembrane protein arranged as a pentamer of alpha helices, which form a channel for ligand binding. In monocytic lineages, TSPO is upregulated during inflammation and is reduced in the presence of anti-inflammatory pharmacotherapies. TSPO has been used as a biomarker particularly for imaging microglia because background TSPO expression in the rest of the central nervous system (CNS) is low. Nevertheless, others have also targeted peripheral macrophage-expressing TSPO to image diseases outside the CNS. A variety of small-molecule TSPO-targeted ligands for PET and SPECT have been developed, such as the first-generation compounds  $^{11}\text{C}$ -PK11195 and  $^{11}\text{C}$ -Ro 5-4864, as well as subsequent radioligands, such as  $^{11}\text{C}$ -DAA1106,<sup>23</sup>  $^{11}\text{C}$ -PBR28,<sup>24</sup> and  $^{11}\text{C}$ -DPA-713.<sup>25</sup> *N,N*-Diethyl-2-[2-(4-methoxy-phenyl)-5,7-dimethyl-pyrazolo[1,5- $\alpha$ ]pyrimidin-3-yl]-acetamide, DPA-713, is a pyrazolopyrimidine that is twice as potent as the first generation, archetypal ligand, PK11195, and 10 times more hydrophilic,<sup>26</sup> allowing for better clearance from nontarget tissues. A drawback of using several second-generation ligands is that binding affinity to TSPO is determined by the subject's genotype (SNP rs6971). High affinity is observed in individuals with two copies coding for alanine at amino acid position 147. Medium affinity is observed in heterozygous individuals, each expressing TSPO containing alanine or threonine, and low affinity is observed in individuals expressing TSPO coding for threonine at position 147.<sup>27</sup> This drawback certainly limits imaging in T/T expressing individuals and reduces sensitivity in individuals expressing A/T when using these radiotracers. (*R*)- $^{11}\text{C}$ -PK11195 exhibits uniform affinity for TSPO

regardless of genotype, but suffers from a characteristic highly lipophilic biodistribution profile in CNS as well as in periphery and leads to high nonspecific background uptake.

Neuroimaging using radiolabeled TSPO ligands is by far the most pursued application of TSPO imaging.<sup>28,29</sup> This technique relies upon the restricted expression of TSPO within the CNS, which is limited to microglia, astrocytes, choroid plexus, and ependymal cells of the ventricles and the olfactory bulb. Disease states involving gliosis, either early-phase microglial activation or chronic astrogliosis, for which TSPO imaging has been employed, include inflammation secondary to contact sport head trauma,<sup>30</sup> inflammation in multiple sclerosis,<sup>31</sup> and inflammation in neuropsychiatric disorders<sup>32</sup> and in a rabbit model of tuberculous meningitis.<sup>33</sup>

Peripheral macrophage imaging via TSPO is possible and has been reported in experimental models of rheumatoid arthritis,<sup>34</sup> atherosclerosis,<sup>35,36</sup> and tumor-associated macrophage imaging.<sup>37</sup> Because of relatively rapid tracer kinetics (0–2 hours post injection), largely because of short radionuclide half-life and high densities of TSPO expression in the lungs, heart, adrenal glands, and kidney, imaging is largely confined to either the extremities or the brain, where background signal is low. One exception to this restriction is the discovery that radioiodinated DPA-713 is almost exclusively retained by macrophages at a longer uptake time (24 hours post injection) while washing out of TSPO-expressing tissues, allowing imaging of macrophages almost anywhere within the CNS or periphery. <sup>125</sup>I-Iodo-DPA-713 was found to accumulate specifically in tuberculosis (TB)-associated inflammatory lesions in murine models.<sup>38</sup> Serial <sup>125</sup>I-DPA-713 SPECT was also able to correctly identify the bactericidal activities of the two TB treatments as early as 4 weeks after the start of treatment.<sup>39</sup> Furthermore, <sup>124</sup>I-DPA-713 PET was able to localize TB lesions with high signal-to-noise ratios (Fig.). However, gastrointestinal clearance of radiotracer makes imaging challenging in this tissue. Lastly, pharmacotherapies applied to the patient may also affect imaging data. Using anti-inflammatory or steroidal medications regardless of source or molecular target may upregulate or downregulate macrophage or microglial inflammation and may result in altered radiotracer uptake.

### **Oxidized LDL Receptor (LOX-1)**

LOX-1 is a 52 kDa type II lectin-like inducible membrane protein that forms a homodimer at the plasma membrane.<sup>40</sup> It is conditionally expressed on endothelial cells, macrophages, neutrophils and smooth muscle cells where the C-terminus binds to oxidized low-density lipoprotein (oxLDL) species and other ligands, such as damaged cells, platelets, and bacteria. Ligand binding subsequently activates several signaling molecules, including nuclear factor- $\kappa$ B, resulting in reactive oxygen species release. In the case of endothelial cells, release of reactive oxygen species causes vessel damage as well as stimulates neovascularization. In the case of macrophages and neutrophils, reactive oxygen species release causes tissue damage and innate immune response against bacteria, fungi, and parasites, and in smooth muscle, tissue damage is the primary result.

LOX-1 has served as a biomarker primarily for initiation and progression of atherosclerosis because of its upregulation in a pro-atherogenic environment, including the presence of hypertension and dyslipidemias.<sup>41</sup> In an oxidizing host environment, low-density lipoprotein

(LDL) transforms into oxLDL within tissues or blood either through acetylation of B100 or direct oxidation of the cholesterol ligand. When oxysterol oxLDL binds to LOX-1 on macrophages, it is internalized via a distinct endosomal pathway from LDL and acetylated oxLDL.<sup>42</sup> Oxysterol oxLDL is metabolized much more slowly than LDL, and as a result, endosomes containing oxLDL fuse with lysosomes that expand to contain substantial stores of oxLDL and LDL, which are visible in foamy macrophages using acid red stain. Increasing oxLDL binding promotes upregulation of LOX-1 expression. Efforts to target and noninvasively visualize densities of LOX-1-expressing foam cells, inflamed endothelium, and inflamed cardiac muscle have exclusively employed LOX-1-targeted antibodies. The first reported study described <sup>99m</sup>Tc-labeled anti-LOX-1 IgG in a rabbit model of atherosclerosis.<sup>43</sup> Ex vivo autoradiographic and fluorescent data showed strong tropism for plaque-associated macrophages, and in vivo SPECT-CT data showed focal uptake in descending aorta. Similarly, another group using indium-111-labeled (and also Gd<sup>3+</sup>) anti-LOX-1 IgG conjugated to liposomes to image plaques in a mouse ApoE<sup>-/-</sup> model of atherosclerosis reported similar findings.<sup>44</sup> This group's antibody-guided probe was similarly bound to macrophages within plaques and showed focal vascular uptake in vivo, as well as very high liver uptake. Small-molecule ligands to LOX-1 have been reported,<sup>45</sup> although none have been labeled for imaging.

## Acknowledgments

This work was supported by the National Institutes of Health Director's Transformative Research Award R01-EB020539 (S.K.J.) and R01-HL131829 (S.K.J.). The funders had no role in the study design, data collection and analysis, decision to publish, or preparation of the manuscript.

## References

1. Yi YS. Folate receptor-targeted diagnostics and therapeutics for inflammatory diseases. *Immune Netw.* 2016; 16:337–343. [PubMed: 28035209]
2. Elnakat H, Ratnam M. Distribution, functionality and gene regulation of folate receptor isoforms: Implications in targeted therapy. *Adv Drug Deliv Rev.* 2004; 56:1067–1084. [PubMed: 15094207]
3. Ross JF, Wang H, Behm FG, et al. Folate receptor type beta is a neutrophilic lineage marker and is differentially expressed in myeloid leukemia. *Cancer.* 1999; 85:348–357. [PubMed: 10023702]
4. Low PS, Henne WA, Doorneweerd DD. Discovery and development of folic-acid-based receptor targeting for imaging and therapy of cancer and inflammatory diseases. *Acc Chem Res.* 2008; 41:120–129. [PubMed: 17655275]
5. Chandrupatla D, Jansen G, Vos R, et al. In-vivo monitoring of anti-folate therapy in arthritic rats using [<sup>18</sup>F]fluoro-PEG-folate and positron emission tomography. *Arthritis Res Ther.* 2017; 19:114. [PubMed: 28569209]
6. Mathias CJ, Lewis MR, Reichert DE, et al. Preparation of <sup>66</sup>Ga- and <sup>68</sup>Ga-labeled Ga(III)-deferoxamine-folate as potential folate-receptor-targeted PET radiopharmaceuticals. *Nucl Med Biol.* 2003; 30:725–731. [PubMed: 14499330]
7. Reddy JA, Xu LC, Parker N, et al. Preclinical evaluation of (<sup>99m</sup>Tc)-EC20 for imaging folate receptor-positive tumors. *J Nucl Med.* 2004; 45:857–866. [PubMed: 15136637]
8. Siegel BA, Dehdashti F, Mutch DG, et al. Evaluation of <sup>111</sup>In-DTPA-folate as a receptor-targeted diagnostic agent for ovarian cancer: Initial clinical results. *J Nucl Med.* 2003; 44:700–707. [PubMed: 12732670]
9. Jager NA, Westra J, Golestani R, et al. Folate receptor-beta imaging using <sup>99m</sup>Tc-folate to explore distribution of polarized macrophage populations in human atherosclerotic plaque. *J Nucl Med.* 2014; 55:1945–1951. [PubMed: 25359878]

10. Turk MJ, Breur GJ, Widmer WR, et al. Folate-targeted imaging of activated macrophages in rats with adjuvant-induced arthritis. *Arthritis Rheum.* 2002; 46:1947–1955. [PubMed: 12124880]
11. Paulos CM, Turk MJ, Breur GJ, et al. Folate receptor-mediated targeting of therapeutic and imaging agents to activated macrophages in rheumatoid arthritis. *Adv Drug Deliv Rev.* 2004; 56:1205–1217. [PubMed: 15094216]
12. Xia W, Hilgenbrink AR, Matteson EL, et al. A functional folate receptor is induced during macrophage activation and can be used to target drugs to activated macrophages. *Blood.* 2009; 113:438–446. [PubMed: 18952896]
13. Kraus VB, McDaniel G, Huebner JL, et al. Direct in vivo evidence of activated macrophages in human osteoarthritis. *Osteoarthritis Cartilage.* 2016; 24:1613–1621. [PubMed: 27084348]
14. Ayala-Lopez W, Xia W, Varghese B, et al. Imaging of atherosclerosis in apolipoprotein e knockout mice: Targeting of a folate-conjugated radiopharmaceutical to activated macrophages. *J Nucl Med.* 2010; 51:768–774. [PubMed: 20395331]
15. Shen J, Chelvam V, Cresswell G, et al. Use of folate-conjugated imaging agents to target alternatively activated macrophages in a murine model of asthma. *Mol Pharm.* 2013; 10:1918–1927. [PubMed: 23641923]
16. Mathias CJ, Wang S, Waters DJ, et al. Indium-111-DTPA-folate as a potential folate-receptor-targeted radiopharmaceutical. *J Nucl Med.* 1998; 39:1579–1585. [PubMed: 9744347]
17. Miller JL, de Wet BJ, Martinez-Pomares L, et al. The mannose receptor mediates dengue virus infection of macrophages. *PLoS Pathog.* 2008; 4:e17. [PubMed: 18266465]
18. Op den Brouw ML, Binda RS, Geijtenbeek TB, et al. The mannose receptor acts as hepatitis B virus surface antigen receptor mediating interaction with intrahepatic dendritic cells. *Virology.* 2009; 393:84–90. [PubMed: 19683778]
19. Gazi U, Martinez-Pomares L. Influence of the mannose receptor in host immune responses. *Immunobiology.* 2009; 214:554–561. [PubMed: 19162368]
20. Movahedi K, Schoonooghe S, Laoui D, et al. Nanobody-based targeting of the macrophage mannose receptor for effective in vivo imaging of tumor-associated macrophages. *Cancer Res.* 2012; 72:4165–4177. [PubMed: 22719068]
21. Put S, Schoonooghe S, Devoogdt N, et al. SPECT imaging of joint inflammation with nanobodies targeting the macrophage mannose receptor in a mouse model for rheumatoid arthritis. *J Nucl Med.* 2013; 54:807–814. [PubMed: 23447654]
22. Bala G, Baudhuin H, Remory I, et al. Evaluation of [99mTc]radiolabeled macrophage mannose receptor-specific nanobodies for targeting of atherosclerotic lesions in mice. *Mol Imaging Biol.* 2017
23. Probst KC, Izquierdo D, Bird JL, et al. Strategy for improved [(11C)DAA1106] radiosynthesis and in vivo peripheral benzodiazepine receptor imaging using microPET, evaluation of [(11C)DAA1106]. *Nucl Med Biol.* 2007; 34:439–446. [PubMed: 17499734]
24. Imaizumi M, Kim HJ, Zoghbi SS, et al. PET imaging with [11C]PBR28 can localize and quantify upregulated peripheral benzodiazepine receptors associated with cerebral ischemia in rat. *Neurosci Lett.* 2007; 411:200–205. [PubMed: 17127001]
25. James ML, Fulton RR, Henderson DJ, et al. Synthesis and in vivo evaluation of a novel peripheral benzodiazepine receptor PET radioligand. *Bioorg Med Chem.* 2005; 13:6188–6194. [PubMed: 16039131]
26. Boutin H, Chauveau F, Thominiaux C, et al. 11C-DPA-713: A novel peripheral benzodiazepine receptor PET ligand for in vivo imaging of neuroinflammation. *J Nucl Med.* 2007; 48:573–581. [PubMed: 17401094]
27. Owen DR, Yeo AJ, Gunn RN, et al. An 18-kDa translocator protein (TSPO) polymorphism explains differences in binding affinity of the PET radioligand PBR28. *J Cereb Blood Flow Metab.* 2012; 32:1–5. [PubMed: 22008728]
28. Rupprecht R, Papadopoulos V, Rammes G, et al. Translocator protein (18 kDa) (TSPO) as a therapeutic target for neurological and psychiatric disorders. *Nat Rev Drug Discov.* 2010; 9:971–988. [PubMed: 21119734]
29. Roncaroli F, Su Z, Herholz K, et al. TSPO expression in brain tumours: Is TSPO a target for brain tumour imaging? *Clin Transl Imaging.* 2016; 4:145–156. [PubMed: 27077069]

30. Coughlin JM, Wang Y, Minn I, et al. Imaging of glial cell activation and white matter integrity in brains of active and recently retired national football league players. *JAMA Neurol.* 2017; 74:67–74. [PubMed: 27893897]
31. Sucksdorff M, Rissanen E, Tuisku J, et al. Evaluation of the effect of fingolimod treatment on microglial activation using serial PET imaging in multiple sclerosis. *J Nucl Med.* 2017; 58:1646–1651. [PubMed: 28336784]
32. Selvaraj S, Bloomfield PS, Cao B, et al. Brain TSPO imaging and gray matter volume in schizophrenia patients and in people at ultra high risk of psychosis: An [11C]PBR28 study. *Schizophr Res.* 2017
33. Tucker EW, Pokkali S, Zhang Z, et al. Microglia activation in a pediatric rabbit model of tuberculous meningitis. *Dis Model Mech.* 2016; 9:1497–1506. [PubMed: 27935825]
34. Pottier G, Bernards N, Dolle F, et al. [(1)(8)F]DPA-714 as a biomarker for positron emission tomography imaging of rheumatoid arthritis in an animal model. *Arthritis Res Ther.* 2014; 16:R69. [PubMed: 24621017]
35. Gaemperli O, Shalhoub J, Owen DR, et al. Imaging intraplaque inflammation in carotid atherosclerosis with 11C-PK11195 positron emission tomography/computed tomography. *Eur Heart J.* 2012; 33:1902–1910. [PubMed: 21933781]
36. Foss CA, Bedja D, Mease RC, et al. Molecular imaging of inflammation in the ApoE  $-/-$  mouse model of atherosclerosis with IodoDPA. *Biochem Biophys Res Commun.* 2015; 461:70–75. [PubMed: 25858322]
37. Zinnhardt B, Pigeon H, Theze B, et al. Combined PET imaging of the inflammatory tumor microenvironment identifies margins of unique radiotracer uptake. *Cancer Res.* 2017; 77:1831–1841. [PubMed: 28137769]
38. Foss CA, Harper JS, Wang H, et al. Noninvasive molecular imaging of tuberculosis-associated inflammation with radioiodinated DPA-713. *J Infect Dis.* 2013; 208:2067–2074. [PubMed: 23901092]
39. Ordonez AA, Pokkali S, DeMarco VP, et al. Radioiodinated DPA-713 imaging correlates with bactericidal activity of tuberculosis treatments in mice. *Antimicrob Agents Chemother.* 2015; 59:642–649. [PubMed: 25403669]
40. Ohki I, Ishigaki T, Oyama T, et al. Crystal structure of human lectin-like, oxidized low-density lipoprotein receptor 1 ligand binding domain and its ligand recognition mode to OxLDL. *Structure.* 2005; 13:905–917. [PubMed: 15939022]
41. Moore KJ, Sheedy FJ, Fisher EA. Macrophages in atherosclerosis: A dynamic balance. *Nat Rev Immunol.* 2013; 13:709–721. [PubMed: 23995626]
42. Lougheed M, Moore ED, Scriven DR, et al. Uptake of oxidized LDL by macrophages differs from that of acetyl LDL and leads to expansion of an acidic endolysosomal compartment. *Arterioscler Thromb Vasc Biol.* 1999; 19:1881–1890. [PubMed: 10446066]
43. Ishino S, Mukai T, Kuge Y, et al. Targeting of lectinlike oxidized low-density lipoprotein receptor 1 (LOX-1) with 99mTc-labeled anti-LOX-1 antibody: Potential agent for imaging of vulnerable plaque. *J Nucl Med.* 2008; 49:1677–1685. [PubMed: 18794262]
44. Li D, Patel AR, Klivanov AL, et al. Molecular imaging of atherosclerotic plaques targeted to oxidized LDL receptor LOX-1 by SPECT/CT and magnetic resonance. *Circ Cardiovasc Imaging.* 2010; 3:464–472. [PubMed: 20442371]
45. Thakkar S, Wang X, Khaidakov M, et al. Structure-based design targeted at LOX-1, a receptor for oxidized low-density lipoprotein. *Sci Rep.* 2015; 5:16740. [PubMed: 26578342]

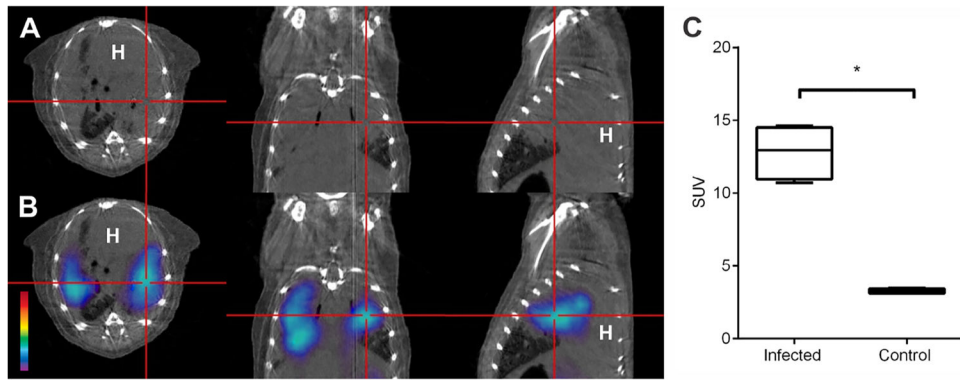


**Figure.** SUV, standardized uptake value; H, heart; \* =  $P < 0.05$ .  $^{124}\text{I}$ -DPA-713 PET imaging of a *Mycobacterium tuberculosis*-infected mouse 24 hours after injection of the tracer. PET signal colocalizes with the pulmonary lesion visualized by CT (panels A and B). PET signal in the pulmonary lesions of infected mice is significantly higher than that in the lungs of uninfected mice. (Adapted from Ordonez et al.<sup>39</sup>)

**Table**Folate Receptor- $\beta$ -targeted In Vivo Imaging

Diseases	Animal Model/Human	Reference
Rheumatoid arthritis	Rat	10
	Dog	11
	Human	12
Osteoarthritis	Human	4,13
Atherosclerosis	Mice	14
Asthma	Mice	15
Ovarian cancer	Human	16

Author Manuscript

Author Manuscript

Author Manuscript

Author Manuscript